JACS
JOURNAL OF THE AMERICAN CHEMICAL SOCIETY
Article
pubs.acs.org/JACS

Surface-Induced Alkene Oligomerization: Does Thermal Hydrosilylation Really Lead to Monolayer Protected Silicon Nanocrystals?

Zhenyu Yang, Muhammad Iqbal, Alexander R. Dobbie, and Jonathan G. C. Veinot*

Department of Chemistry, University of Alberta, Edmonton, Alberta T6G 2G2, Canada

Supporting Information

ABSTRACT: Surface functionalization of hydride-terminated silicon nanocrystals (SiNCs) with dodecene via thermal hydrosilylation has been reexamined. We observed the formation of dodecyl oligomers ($n \leq 4$) during the reaction under an argon atmosphere at various predesigned temperatures (100−190 °C). In a comparative study, surface hydrosilylation and ligand oligomerization were found to be more pronounced under air ($n \leq 7$) at the same temperatures. These observations strongly suggest that hydrogen abstraction by oxygen accelerates hydrosilylation and generates sufficient silyl radical as initiator to interact with unsaturated bonds, promote chain propagation, and generate ligand oligomers. We further propose that, to inhibit ligand oligomerization and obtain monolayer coverage on SiNC surfaces, it is feasible to apply comparatively low temperatures, inert atmosphere, and dilute ligand concentration during thermal hydrosilylation.

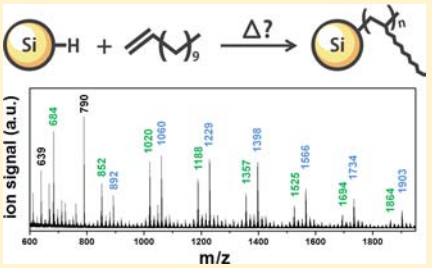

1. INTRODUCTION

Silicon nanocrystals (SiNCs) are intriguing materials because their properties differ substantially from those of their bulk counterparts.[1−3] Their tunable optoelectronic response, as well as low toxicity and biocompatibility, has garnered much attention, and prototype applications including light-emitting diodes, solar cells, and biological probes have been demonstrated.[4−7] Claims have also been made that hydride-terminated SiNCs can "split water" without any energy input.[8] While some exceptions exist,[9−12] most methods to prepare functionalized SiNCs begin with particles terminated with Si−H moieties that are, in turn, modified using various hydrosilylation strategies based upon widely known work on bulk and porous silicon.[13−19] These procedures provide alkyl and alkenyl surface groups that render SiNCs environmentally stable and compatible with common organic solvents. Broadly, hydrosilylation reactions add an Si−H bond across the C−C multiple bond; however, the exact mechanism depends upon the conditions employed (e.g., thermal initiation, photochemical activation, metal-based catalysis, among others).

For reactions on bulk silicon surfaces, Linford and Chidsey have proposed that the reaction proceeds via a self-propagating chain reaction that leads to close-packed monolayers.[14] Investigations probing these reactions under somewhat "ideal" ultra-high-vacuum (UHV) conditions with low monomer concentration, flat single-crystal surfaces, and single initiation sites support this mechanism.[20−22] Subsequently, numerous contributions have reported that analogous surface passivation of silicon nanostructures (e.g., porous silicon, SiNCs) provides close packing of ligands.[17,23−25] Still, the exact hydrosilylation mechanism remains elusive and the subject of ongoing discussions.[25−30] Unquestionably, typical reaction conditions are far from the ideal UHV scenario noted above, and the reaction pathways depend upon the experimental parameters employed. Among the various approaches, thermally initiated hydrosilylation is widely employed for SiNCs because it is not influenced by particle size and shape,[14,15,31,32] it affords comparatively high yields, and there is no need to remove trace catalyst impurities. A commonly accepted thermal hydrosilylation mechanism requires sufficient heat ($T \geq 150$ °C) to homolytically cleave Si−H bonds to create silyl radicals that subsequently react with solution-borne terminal alkenes or alkynes. Once initiated, it is assumed the reaction propagates via a surface chain reaction similar to that proposed for bulk systems.[14] However, thermal hydrosilylation can occur at much lower temperatures (e.g., 110 °C[31]), suggesting Si−H thermal cleavage is not the only mode of activation. Woods et al. invoked a kinetic model for hydrosilylation in which reaction initiation occurs via hydrogen abstraction by trace oxygen to explain low-temperature initiation.[26]

Regardless of the mode of initiation, surface silyl radicals react with unsaturated C−C bonds. To date, it has been reasonably assumed that these reactions yield monolayer coatings. However, faceted and curved surfaces of SiNCs differ substantially from *ideal* bulk Si substrates, solution-phase reactions with SiNCs are pseudo-homogeneous vs heterogeneous for bulk surfaces, and typical concentrations of reagents bearing unsaturated C−C bonds are very high.[33,34] Given these differences, it is possible that surface silyl radicals formed in the initial stages of thermally induced reactions could lead to a variety of products. An important consideration that is largely

Received: September 17, 2013
Published: October 28, 2013

   dx.doi.org/10.1021/ja409657y | J. Am. Chem. Soc. 2013, 135, 17595−17601

absent from the discussion is that of oligomerization (or polymerization) of unsaturated solution species (e.g., alkenes) leading to surface-bonded oligomers (or polymers). It has been revealed that silane molecules are efficient initiators for the polymerization of acrylate systems.[35] In this context, it is important to recall the exceptionally high resolution imaging of SiNCs by transmission electron microscopy (TEM) reported by Panthani et al.[36] that suggests particles may be covered by multilayers or polymerics. Similarly, our group recently reported the preparation of covalently linked SiNC/polystyrene hybrids obtained from thermal hydrosilylation conditions.[37]

Herein, we describe the results of a methodical investigation that was designed to critically examine the products from the thermally induced hydrosilylation of SiNCs by exploring the influence of reaction temperature and atmosphere (i.e., dry argon vs air). Using well-established protocols developed in our laboratory, we prepared oxide-free, surface hydride-terminated SiNCs with different sizes upon HF etching of a hydrogen silsesquioxane-derived $SiNC/SiO_2$ composite.[32,38] SiNC surfaces were subsequently functionalized via a thermally initiated hydrosilylation. Dodecene was chosen as the alkene of choice because it affords a wide reaction temperature range bracketing that required for Si−H cleavage (i.e., 80−190 °C). Reaction progress is qualitatively evaluated by monitoring the visual transparency of the reaction mixture, which started as a cloudy yellow suspension and became transparent orange. Products were purified and evaluated using infrared (IR) and photoluminescence (PL) spectroscopy, X-ray photoelectron spectroscopy (XPS), and mass spectrometry (MS).

2. EXPERIMENTAL SECTION

Reagents and Materials. Hydrogen silsesquioxane (HSQ_8 trade name Fox-17, sold commercially as a solution in methyl isobutyl ketone) was purchased from Dow Corning Corp. (Midland, MI). Electronic-grade hydrofluoric acid (HF, 49% aqueous solution) was purchased from J. T. Baker. Methanol (reagent grade), toluene (reagent grade), ethanol (reagent grade), 1-dodecene (97%), and dodecane (99%) were purchased from Sigma-Aldrich and used as received.

Preparation of Oxide-Embedded Silicon Nanocrystals (d = 3 nm). The solvent was removed from the stock HSQ_8 solution under vacuum to yield white solid powders. HSQ_8 solid (ca. 4 g) was placed in a quartz reaction boat, transferred to a Lindberg Blue tube furnace, and heated from ambient to a peak processing temperature of 1100 °C at 18 °C min^{-1} in a slightly reducing atmosphere (5% H_2/95% Ar). The sample was maintained at the peak processing temperature for 1 h. Upon cooling to room temperature, the resulting amber solid was ground into a fine brown powder using a two-step process. First, the solid was crushed using an agate mortar and pestle to remove large particles. Further grinding was achieved using a Burrell wrist-action shaker upon shaking with high-purity silica beads for 5 h. The resulting $SiNC/SiO_2$ composite powders were stable for extended periods and stored in standard glass vials.

Preparation of Oxide-Embedded Silicon Nanocrystals (d = 5 and 8 nm). Following mortar and pestle grinding (*vide supra*), 0.5 g of $SiNC/SiO_2$ composite containing 3 nm SiNCs was transferred to a high-temperature furnace (Sentro Tech Corp.) for further thermal processing in an argon atmosphere. This procedure leads to particle growth while maintaining relatively narrow particle size distributions. In the furnace, the $SiNC/SiO_2$ composite was heated to appropriate peak processing temperatures at 10 °C/min to achieve the target particle size (i.e., 1200 °C for 5 nm NCs and 1300 °C for 8 nm NCs). Samples were maintained at the peak processing temperature for 1 h. After cooling to room temperature, the brown composites were ground using procedures identical to those noted above.

Liberation of SiNCs. Hydride-terminated SiNCs were liberated from the $SiNC/SiO_2$ composites using HF etching. First, 0.2 g of the ground $SiNC/SiO_2$ composite was transferred to a polyethylene terephthalate beaker equipped with a Teflon-coated stir bar. Ethanol (3 mL) and water (3 mL) were then added under mechanical stirring to form a brown suspension, followed by 3 mL of 49% HF aqueous solution. (***Caution!*** *HF must be handled with extreme care.*) After 1 h of etching in subdued light, the suspension appeared orange/yellow. Hydride-terminated SiNCs were subsequently extracted from the aqueous layer into ca. 30 mL of toluene by multiple (i.e., 3 × 10 mL) extractions. The SiNC toluene suspension was transferred to test tubes, and the SiNCs were isolated by centrifugation at 3000 rpm.

Thermal Functionalization of Dodecyl-Modified SiNCs. After decanting the toluene supernatant, the resulting hydride-terminated particles were redispersed into ca. 20 mL of dodecene to yield a cloudy suspension, which was transferred to a dry 100 mL Schlenk flask equipped with a magnetic stir bar and attached to a Schlenk line. The flask was evacuated and backfilled with argon three times to remove air and residual toluene from the solution. The temperature was increased to the set processing temperatures (i.e., 100, 120, 140, 160, and 190 °C, respectively), and the reaction was left stirring for a minimum of 15 h. For those comparison reactions in air atmosphere, the flask was reconnected to air atmosphere before the heating process.

Thermal Functionalization of SiNCs with Diluted Dodecene Solution. The dodecene was diluted by dodecane to form two solutions with different concentration: (1) 5 mL of dodecene/15 mL of dodecane and (2) 2.5 mL of dodecene/17.5 mL of dodecane. Following the extraction and centrifugation (*vide supra*), hydride-terminated SiNCs were redispersed into these solutions, respectively. The mixed solution, which was cloudy yellow, was further transferred to a dry 100 mL Schlenk flask equipped with a magnetic stir bar and attached to a Schlenk line. Similarly, the flask was evacuated and backfilled with argon three times. The temperature was set at 190 °C, and the reaction was left stirring for a minimum of 15 h.

SiNC Purification. Following thermal hydrosilylation, the solution was evenly dispensed into 1.5 mL centrifuge tubes (ca. 0.3 mL each). Next, ca. 1.2 mL of 1:1 methanol/ethanol mixture was added into each tube, resulting in a cloudy yellow dispersion. The precipitate was isolated by centrifugation in a high-speed centrifuge at 17 000 rpm for 15 min. The supernatant was decanted, and the particles were redispersed in a minimum amount of toluene and subsequently precipitated by addition of the 1:1 methanol/ethanol again. The centrifugation and decanting procedure was repeated twice. Finally, the purified-functionalized SiNCs were redispersed in toluene, filtered through a 0.45 μm PTFE syringe filter, and stored in vials for further use.

Control Samples. First, 10 mL of neat dodecene was transferred to a dry 100 mL Schlenk flask equipped with a magnetic stir bar and attached to a Schlenk line. The flask was evacuated and backfilled with argon three times. The temperature was then increased similarly to the thermal hydrosilylation reactions (*vide supra*, i.e., 100, 120, 140, 160, and 190 °C, respectively) for a minimum of 15 h. For those control samples heated under air atmosphere, the flask was reconnected to air atmosphere before the heating process.

Material Characterization and Instrumentation. PL spectra were obtained by irradiation of a quartz vial containing the sample toluene solution with a 441 nm line of a GaN laser. Emitted photons were collected with a fiber optic connected to an Ocean Optics USB2000 spectrometer. Fourier transform (FT)-IR spectroscopy was performed on powder samples using a Nicolet Magna 750 IR spectrophotometer. X-ray photoelectron spectra were acquired in energy spectrum mode at 210 W, using a Kratos Axis Ultra X-ray photoelectron spectrometer. Samples were prepared as films drop-cast from solution onto a copper foil substrate. For nanostructure-assisted laser desorption/ionization (NALDI)-MS sample preparation, 1 μL of the sample solution was spotted onto a Bruker Daltonics NALDI target and air-dried. Mass spectra were obtained in the positive/negative reflectron mode using a Bruker Daltonics (Bremen, Germany) UltrafleXtreme MALDI TOF/TOF mass spectrometer.

EI-MS spectra were recorded on a Kratos MS-50 (high resolution, electron impact ionization). Samples were loaded by direct probe.

3. RESULTS AND DISCUSSION

FT-IR analysis is the most commonly employed method for evaluating SiNCs surface modification and provides valuable information regarding covalent attachment of the surface groups. The FT-IR spectrum of Si−H-terminated SiNCs (Figure 1a) shows strong absorptions attributed to Si−H_x

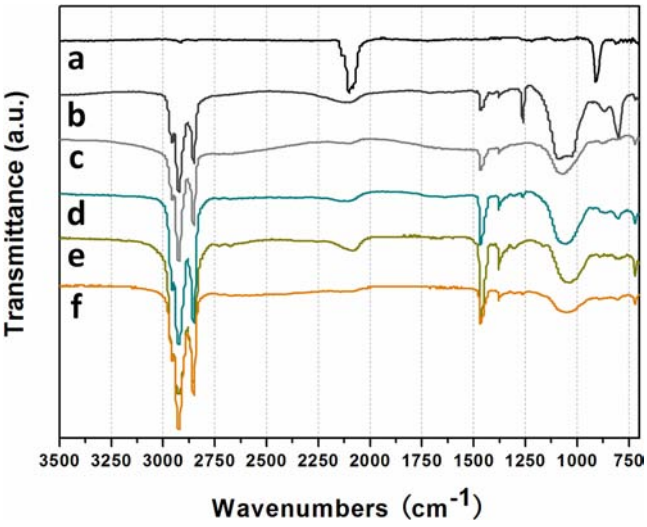

Figure 1. FT-IR spectra of 3 nm (a) hydride-terminated and (b−f) dodecyl-passivated Si functionalized under argon atmosphere at various temperatures: (b) 100, (c) 120, (d) 140, (e) 160, and (f) 190 °C.

(ca. 2100 and 850 cm^{-1}, respectively). Following hydrosilylation (see Figure 1), absorptions associated with Si−H are replaced by intense vibrations at 2650−2900 and 1380−1470 cm^{-1}, characteristic of alkyl functionalities and consistent with surface modification.[32] Of particular importance to the present discussion, these features cannot be used to distinguish among monolayers, oligomers, or polymers. Weak absorptions at ca. 1100 cm^{-1} are also observed that indicate some limited surface oxidation of SiNCs has occurred. The oxidation state(s) of the SiNC cores was evaluated using XPS (Figure 2). An emission at 99.3 eV routinely attributed to Si(0) was noted, while other components at 100.3, 101.3, 102.4, and 103.4 eV were assigned to the functionalized surface atoms as well as Si sub-oxides.

MS was employed to evaluate the identity of SiNC surface groups. In light of the strong covalent Si−C bonds that bind the alkyl-based moieties to the SiNCs, NALDI was employed. The MS data for functionalized particles obtained from a reaction performed at 190 °C under inert Ar atmosphere are shown in Figure 3. No fragments associated with the molecular weight of dodecene (MW = 168.3) were detected, consistent with effective purification. The fragmentation pattern observed is complex; however, this is not unexpected when comparing the various bond strengths at the SiNC surface (i.e., Si−Si, 210−250; Si−C, 369; and C−C, 292−360 kJ mol^{-1}).[39] Because the Si−Si linkage is the weakest of the surface bonds, it will cleave preferentially, and liberated groups are expected to include differing numbers of silicon atoms. This complexity precludes definitive assignment of individual MS signals. Still, important insight into the nature of the SiNC surface species can be obtained when considering series of signals that are

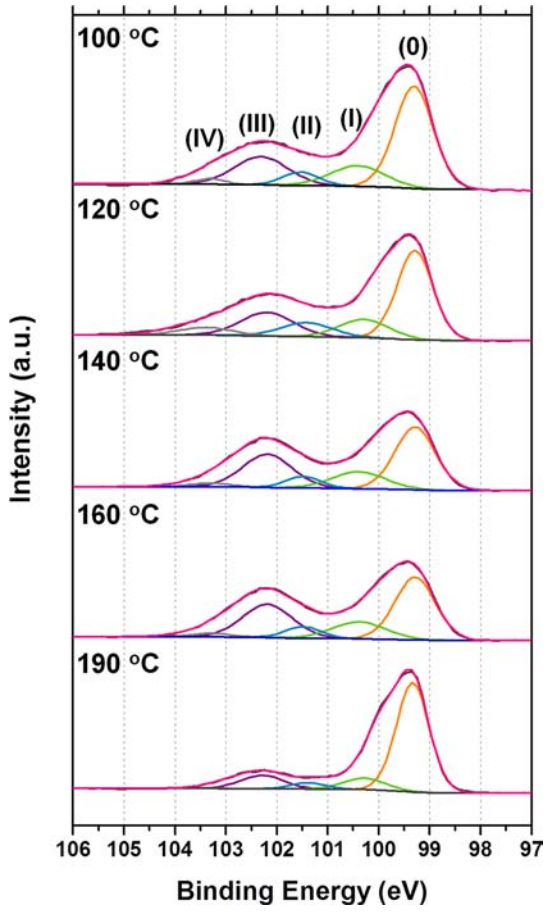

Figure 2. High-resolution XPS spectra of silicon (2p) for dodecyl-passivated SiNCs functionalized under Ar atmosphere at various temperatures (100−190 °C). Fitting results are shown for the silicon spectrum with Si $2p_{3/2}$ signal. The Si $2p_{1/2}$ signals have been removed for clarity.

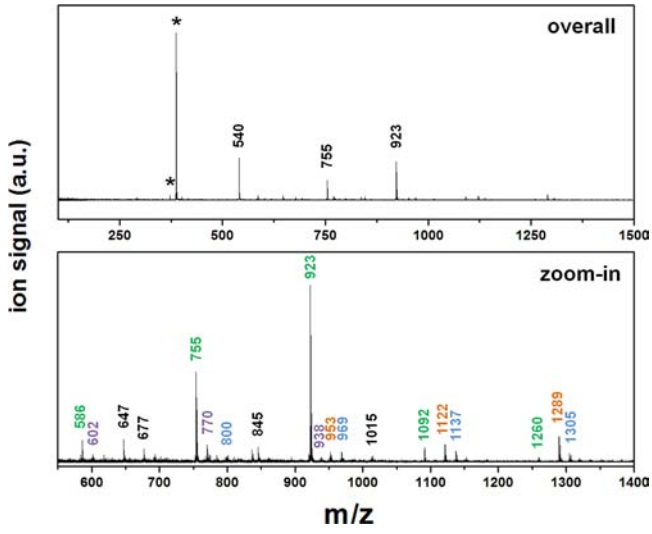

Figure 3. NALDI mass spectra of 3 nm dodecyl-passivated SiNCs functionalized at 190 °C under argon. Numbers in different colors indicate the gap corresponding to a dodecene unit (i.e., m/z = 168.3). Numbers in black are assigned to unspecific fragments. Asterisks indicate background signal.

separated by m/z = 168.3, consistent with the loss of a dodecyl repeat unit from an oligomer or polymer. Further evaluation of

dx.doi.org/10.1021/ja409657y | J. Am. Chem. Soc. 2013, 135, 17595−17601

the fragmentation pattern suggests that species liberated from the NC surfaces consist of two (purple and orange labels), three (blue labels), and four (green labels) dodecyl repeat units, consistent with surface oligomerization. Even more telling, when a blank sample (i.e., pure dodecene, without SiNCs) was also heated following the identical procedure, only a trace amount of dimer (i.e., MW = 336.4) was detected (Figure S1). These observations suggest that high-temperature functionalization of hydride-terminated SiNCs with alkenes leads to ligand oligomerization.

Based upon the generally accepted mechanism that involves the homolytic cleavage of the Si−H bond, it is expected that reaction temperature will play a crucial role in thermal hydrosilylation. By extension, temperature is certainly a key factor in the formation of oligomers. In this context, we explored how changes in reaction temperature impacted the product distribution for reactions carried out at predetermined temperatures between 80 and 160 °C. With heating to 80 °C, no qualitative changes in the appearance of the reaction mixture were noted, even after prolonged (i.e., 3 days) heating. This observation is expected, given that homolytic cleavage of Si−H requires temperatures of at least 150 °C.[39] To our surprise, reactions performed at 100 °C afforded transparent orange SiNC solutions after 72 h; when they were heated to 120 and 140 °C, only 15 h was required. Removal of solvent provided a dark brown powder. IR and XPS analyses of samples prepared at 100, 120, and 140 °C confirmed surface functionalization and limited oxidation (Figures 1 and 2). No obvious evidence of ligand oligomerization was detected in the NALDI-MS analysis of products from reactions heated to 100 °C, suggesting monolayer formation. Spectral signatures of products prepared at 120 and 140 °C (Figures 4 and S2) do suggest oligomerization. More specifically, samples prepared at 120 °C show a series of four peaks separated by 168.3 (green labels in Figure 4), consistent with the presence of dodecyl trimers. Similarly, products from reactions at 140 and 160 °C show peaks separated by 168.3. Again, neat dodecene was heated under identical conditions, and only signals attributable to the monomer were detected (Figure S1), indicating that oligomer formation relies upon the presence of the SiNCs and the hydrosilylation process.

Our observations, that thermally induced hydrosilylation of SiNC surfaces occurs in ambient and subdued light at $100 \leq T \leq 140$ °C, contradict the widely accepted mechanism involving the thermally induced formation of silyl radicals via homolytic cleavage of surface Si−H bonds.[39] One explanation for our findings was proposed by Woods et al., who considered hydrogen abstraction by trace oxygen while simulating a kinetic model for the hydrosilylation initiation step.[26] Those authors found that the computationally determined activation energy was much lower when trace oxygen was considered. This is in good agreement with our observations of low-temperature hydrosilylation and supports the hypothesis that hydrogen abstraction is another initiation pathway. In the context of our observations, we provide a possible mechanism of thermal hydrosilylation/oligomerization (see Scheme 1). We propose two reasonable modes of initiation: homolytic cleavage and hydrogen abstraction. Subsequently, the surface dangling bond (or silyl radical) reacts with a terminal alkene, producing a Si−C linkage and a secondary radical that reacts with additional terminal alkenes, leading to chain propagation and the formation of a surface-bonded oligomer. Because there is no evidence of oligomers in our control dodecene samples

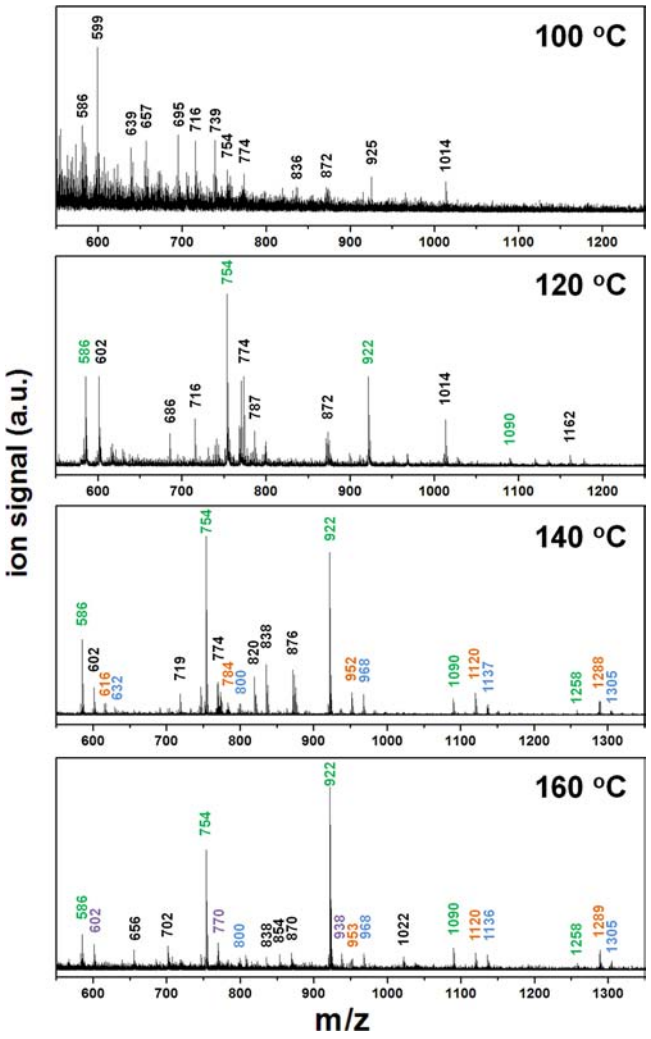

Figure 4. Zoom-in NALDI mass spectra of 3 nm dodecyl-passivated SiNCs functionalized at different temperatures under argon. Numbers in different colors indicate the gap corresponding to a dodecene unit (i.e., m/z = 168.3). Numbers in black are attributed to unidentified fragments.

Scheme 1. Proposed Mechanism of Thermal Hydrosilylation and Ligand Oligomerization Processed at Different Temperatures, Involving Homolytic Cleavage of Si−H Bond and Hydrogen Abstraction by Oxygen

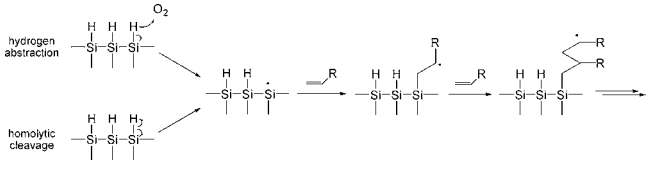

prepared at <190 °C, it is clear that the silyl radical is crucial for ligand oligomerization. This is further supported by our observations that more and longer oligomers are detected in the samples functionalized at higher temperatures.

If the silyl radical is responsible for the formation of oligomers, then reaction of Si−H-terminated SiNCs with dodecene in the presence of oxygen should lead to more oligomerization. To elucidate this potential "oxygen effect" on hydrosilylation/oligomerization, we performed thermal-induced hydrosilylation in air. Potential nitrogen influence is

simply excluded by control tests, whose results are similar to those obtained by reactions under Ar. Reactions performed at 100 °C provided only surface-oxidized SiNCs. Upon increasing the reaction temperature to 120 °C, partially functionalized SiNCs bearing alkyl-based ligands and surface oxide were obtained. It is not surprising that silicon surfaces get oxidized when exposed to air; however, when the reaction was performed at higher temperatures, hydrosilylation proceeded qualitatively more quickly (i.e., 140 °C, ca. 3 h; 160 °C, ca. 1 h; 190 °C, ca. 30 min.) than the identical reactions carried in an argon atmosphere. The resulting products were obtained as photoluminescent transparent orange solutions. Unlike samples prepared in Ar atmosphere (*vide supra*), these solutions afforded a viscous orange oil upon solvent removal. IR spectra (Figure S3) confirmed effective passivation with alkyl chains and suggested that the degree of surface oxidation decreases with higher temperature, as evidenced by Si−O−Si stretching at ca. 1100 cm^{-1}. Detailed XPS analysis of the Si oxidation states for samples obtained at 140, 160, and 190 °C are shown (Figure S4). Not unexpectedly, oxide components are more dominant than those obtained from samples reacted under Ar, and, consistent with our IR data, we note a decrease in oxidation with higher reaction temperature. As anticipated, a slight blue-shift was observed in PL spectra (Figure 5), which

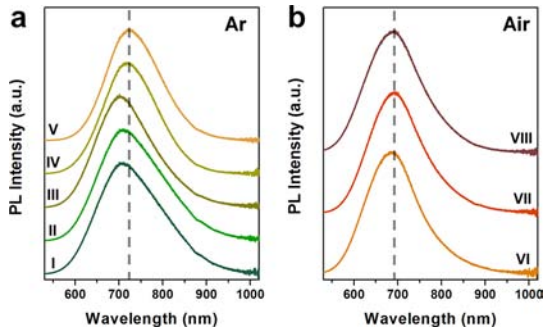

Figure 5. PL spectra of 3 nm dodecyl functionalized under (a) argon and (b) air environments at various processing temperatures: (I) 100, (II) 120, (III,VI) 140, (IV,VII) 160, and (V,VIII) 190 °C. Dotted lines indicate the wavelength value corresponding to peak maxima of spectra V and VIII.

could be assigned to surface oxidation states, as reported in the literature.[40,41] The observation of faster hydrosilylation in air at higher temperature supports the proposition of an initiation pathway involving silyl radical formation by oxygen abstraction. Furthermore, the present observations that functionalization does not occur at lower temperature (i.e., 100 and 120 °C) suggest a competitive relationship between the oxidation and hydrosilylation reactions and that higher temperature favors hydrosilylation.

Again, NALDI-MS analysis of the functionalized SiNCs showed no signals attributed to free dodecene monomer, and there was clear indication of dodecene oligomers (Figures 6 and S5). Similar to our inert atmosphere functionalization, when air is included in the reaction, we note that a higher reaction temperature generates more and longer dodecyl oligomers (i.e., up to $n = 7$). Comparing the products obtained from inert and air reaction atmospheres, we find that air provides longer oligomer chains (i.e., $n_{air} = 7$ vs $n_{Ar} = 4$). As was the case with all dodecene controls, no oligomer was detected by EI-MS upon heating to 140 °C in the absence of hydride-

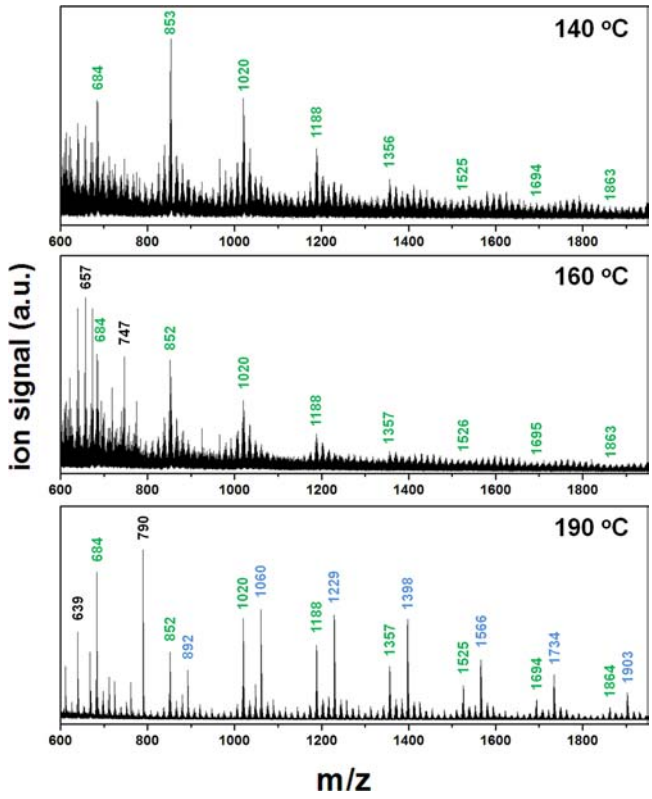

Figure 6. Zoom-in NALDI mass spectra of 3 nm dodecyl-passivated SiNCs functionalized at different temperatures under an air atmosphere.

terminated SiNCs; trace quantities of dimer and trimer were detected after heating to 160 and 190 °C, respectively (Figure S6). These control samples clearly highlight the role of Si−H-terminated SiNCs in dodecene oligomerization.

Having identified that surface functionalization of SiNCs via thermal hydrosilylation yields complex mixtures of surface products, we endeavored to identify if this reaction exhibited a size dependence. In this regard, we performed reactions with $d = 5$ and 8 nm SiNCs in dodecene and observed identical trends associated with oligomer formation, reaction temperature, and atmosphere (Figures 7 and S7). We also discovered that decreasing the dodecene concentration led to lower oligomer production. When reactions were performed at 190 °C in argon using dodecene diluted with dodecane (i.e., 5 mL of dodecene in 15 mL of dodecane, and 2.5 mL of dodecene in 17.5 mL of dodecane), we noted a marked decrease in oligomer formation (Figure S8).

4. CONCLUSION

In conclusion, the present study is the first reported detailed investigation into the nature of the surface species on free-standing SiNCs obtained from thermally induced hydrosilylation. We show convincing evidence that ligand oligomerization occurs under a variety of conditions and confirm that hydrogen abstraction by oxygen enables hydrosilylation to proceed at lower temperature through the production of silyl radicals. The resulting silyl radicals react with the unsaturated C═C bond, which subsequently promotes chain propagation and ultimately generates ligand oligomers on SiNC surfaces. These findings are supported by similar reactions under an air atmosphere, in which both rate of reaction and amount of

dx.doi.org/10.1021/ja409657y | J. Am. Chem. Soc. 2013, 135, 17595−17601

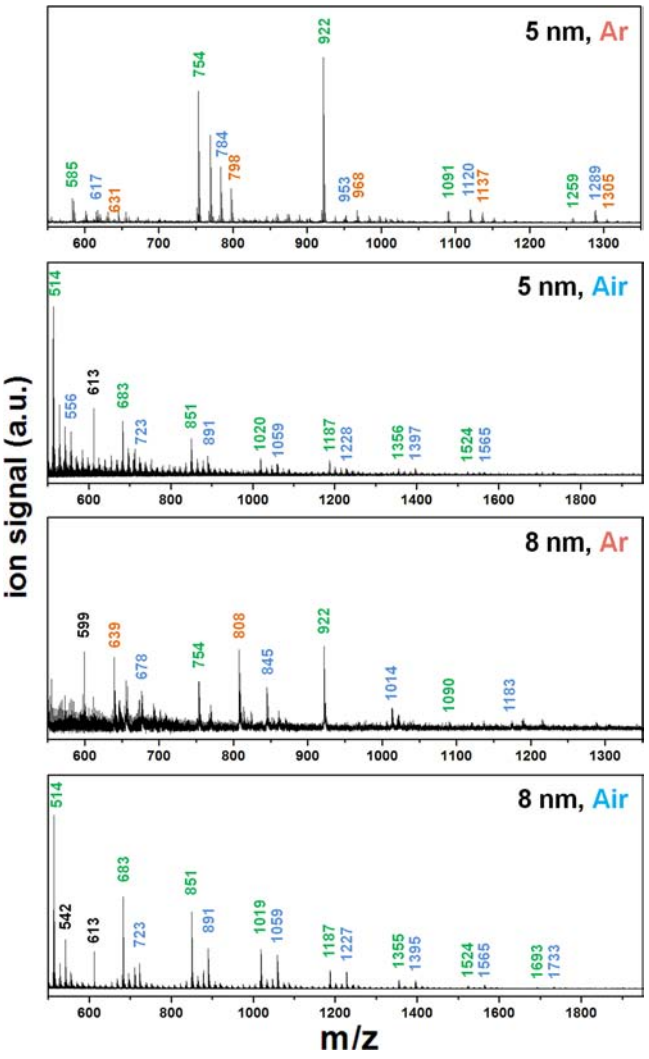

Figure 7. Zoom-in NALDI mass spectra of 5 and 8 nm dodecyl-passivated SiNCs functionalized at 190 °C under argon and air atmosphere. Numbers in different colors indicate the gap corresponding to a dodecene unit. Numbers in black are attributed to unidentified fragments.

surface oligomers increased. Based on this systematic study, it is clear that comparatively low temperature, inert atmosphere, and dilute ligand concentration are crucial to limit surface oligomerization and to obtain monolayer surface coverage.

■ ASSOCIATED CONTENT

Ⓢ Supporting Information

Experimental details and additional characterizations of SiNCs functionalized under argon and air atmosphere. This material is available free of charge via the Internet at http://pubs.acs.org.

■ AUTHOR INFORMATION

Corresponding Author

jveinot@ualberta.ca

Notes

The authors declare no competing financial interest.

■ ACKNOWLEDGMENTS

The authors acknowledge funding from the Natural Sciences and Engineering Research Council of Canada (NSERC), Canada Foundation for Innovation (CFI), Alberta Science and Research Investment Program (ASRIP), and University of Alberta Department of Chemistry. We thank W. C. Moffat, M. Skjel, and M. Hoyle for assistance with FT-IR spectroscopy analysis. The staff at the Alberta Centre for Surface Engineering and Sciences (ACSES) and Mass Spectrometry Laboratory are thanked for XPS and MS analysis. We also thank R. A. Lockwood and Dr. A. Meldrum for assistance with PL measurements. All Veinot Team members are also thanked for useful discussions.

■ REFERENCES

(1) Brus, L. *J. Phys. Chem.* **1994**, *98*, 3575−3581.
(2) Ding, Z.; Quinn, B. M.; Haram, S. K.; Pell, L. E.; Korgel, B. A.; Bard, A. J. *Science* **2002**, *296*, 1293−1297.
(3) Heitmann, J.; Müller, F.; Zacharias, M.; Gösele, U. *Adv. Mater.* **2005**, *17*, 795−803.
(4) Zhong, Y.; Peng, F.; Bao, F.; Wang, S.; Ji, X.; Yang, L.; Su, Y.; Lee, S.-T.; He, Y. *J. Am. Chem. Soc.* **2013**, *135*, 8350−8356.
(5) Liu, J.; Erogbogbo, F.; Yong, K.-T.; Ye, L.; Liu, J.; Hu, R.; Chen, H.; Hu, Y.; Yang, Y.; Yang, J.; Roy, I.; Karker, N. A.; Swihart, M. T.; Prasad, P. N. *ACS Nano* **2013**, *7*, 7303−7310.
(6) Cheng, K.-Y.; Anthony, R.; Kortshagen, U. R.; Holmes, R. J. *Nano Lett.* **2010**, *10*, 1154−1157.
(7) Jang, H.; Pell, L. E.; Korgel, B. A.; English, D. S. *J. Photochem. Photobiol. A* **2003**, *158*, 111−117.
(8) Erogbogbo, F.; Lin, T.; Tucciarone, P. M.; LaJoie, K. M.; Lai, L.; Patki, G. D.; Prasad, P. N.; Swihart, M. T. *Nano Lett.* **2013**, *13*, 451−456.
(9) Bley, R. A.; Kauzlarich, S. M. *J. Am. Chem. Soc.* **1996**, *118*, 12461−12462.
(10) Liu, Q.; Kauzlarich, S. M. *Mater. Sci. Eng., B* **2002**, *96*, 72−75.
(11) Rowsell, B. D.; Veinot, J. G. C. *Nanotechnology* **2005**, *16*, 732−736.
(12) Heintz, A. S.; Fink, M. J.; Mitchell, B. S. *Adv. Mater.* **2007**, *19*, 3984−3988.
(13) Linford, M. R.; Chidsey, C. E. D. *J. Am. Chem. Soc.* **1993**, *115*, 12631−12632.
(14) Linford, M. R.; Fenter, P.; Eisenberger, P. M.; Chidsey, C. E. D. *J. Am. Chem. Soc.* **1995**, *117*, 3145−3155.
(15) Boukherroub, R.; Morin, S.; Bensebaa, F.; Wayner, D. D. M. *Langmuir* **1999**, *15*, 3831−3835.
(16) Cicero, R. L.; Linford, M. R.; Chidsey, C. E. D. *Langmuir* **2000**, *16*, 5688−5695.
(17) Stewart, M. P.; Buriak, J. M. *J. Am. Chem. Soc.* **2001**, *123*, 7821−7830.
(18) Sun, Q.-Y.; de Smet, L. C. P. M.; van Lagen, B.; Giesbers, M.; Thüne, P. C.; van Engelenburg, J.; de Wolf, F. A.; Zuilhof, H.; Sudhölter, E. J. R. *J. Am. Chem. Soc.* **2005**, *127*, 2514−2523.
(19) Tilley, R. D.; Yamamoto, K. *Adv. Mater.* **2006**, *18*, 2053−2056.
(20) Lopinski, G. P.; Wayner, D. D. M.; Wolkow, R. A. *Nature* **2000**, *406*, 48−51.
(21) Cicero, R. L.; Chidsey, C. E. D.; Lopinski, G. P.; Wayner, D. D. M.; Wolkow, R. A. *Langmuir* **2001**, *18*, 305−307.
(22) DiLabio, G. A.; Piva, P. G.; Kruse, P.; Wolkow, R. A. *J. Am. Chem. Soc.* **2004**, *126*, 16048−16050.
(23) Sieval, A. B.; Demirel, A. L.; Nissink, J. W. M.; Linford, M. R.; van der Maas, J. H.; de Jeu, W. H.; Zuilhof, H.; Sudhölter, E. J. R. *Langmuir* **1998**, *14*, 1759−1768.
(24) Rosso-Vasic, M.; Spruijt, E.; van Lagen, B.; De Cola, L.; Zuilhof, H. *Small* **2008**, *4*, 1835−1841.
(25) Boukherroub, R.; Morin, S.; Wayner, D. D. M.; Bensebaa, F.; Sproule, G. I.; Baribeau, J. M.; Lockwood, D. J. *Chem. Mater.* **2001**, *13*, 2002−2011.
(26) Woods, M.; Carlsson, S.; Hong, Q.; Patole, S. N.; Lie, L. H.; Houlton, A.; Horrocks, B. R. *J. Phys. Chem. B* **2005**, *109*, 24035−24045.
(27) Eves, B. J.; Lopinski, G. P. *Langmuir* **2006**, *22*, 3180−3185.

(28) Mischki, T. K.; Lopinski, G. P.; Wayner, D. D. M. *Langmuir* **2009**, *25*, 5626−5630.
(29) Wang, X.; Ruther, R. E.; Streifer, J. A.; Hamers, R. J. *J. Am. Chem. Soc.* **2010**, *132*, 4048−4049.
(30) Coletti, C.; Marrone, A.; Giorgi, G.; Sgamellotti, A.; Cerofolini, G.; Re, N. *Langmuir* **2006**, *22*, 9949−9956.
(31) Bateman, J. E.; Eagling, R. D.; Worrall, D. R.; Horrocks, B. R.; Houlton, A. *Angew. Chem., Int. Ed.* **1998**, *37*, 2683−2685.
(32) Yang, Z.; Dobbie, A. R.; Cui, K.; Veinot, J. G. C. *J. Am. Chem. Soc.* **2012**, *134*, 13958−13961.
(33) Song, J. H.; Sailor, M. J. *J. Am. Chem. Soc.* **1998**, *120*, 2376−2381.
(34) Kelly, J. A.; Henderson, E. J.; Clark, R. J.; Hessel, C. M.; Cavell, R. G.; Veinot, J. G. C. *J. Phys. Chem. C* **2010**, *114*, 22519−22525.
(35) Lalevee, J.; Dirani, A.; El-Roz, M.; Allonas, X.; Fouassier, J. P. *Macromolecules* **2008**, *41*, 2003−2010.
(36) Panthani, M. G.; Hessel, C. M.; Reid, D.; Casillas, G.; José-Yacamán, M.; Korgel, B. A. *J. Phys. Chem. C* **2012**, *116*, 22463−22468.
(37) Yang, Z.; Dasog, M.; Dobbie, A. R.; Lockwood, R.; Zhi, Y.; Meldrum, A.; Veinot, J. G. C. *Adv. Funct. Mater.* **2013**, DOI: 10.1002/adfm.201302091.
(38) Hessel, C. M.; Reid, D.; Panthani, M. G.; Rasch, M. R.; Goodfellow, B. W.; Wei, J.; Fujii, H.; Akhavan, V.; Korgel, B. A. *Chem. Mater.* **2011**, *24*, 393−401.
(39) Buriak, J. M. *Chem. Rev.* **2002**, *102*, 1271−1308.
(40) Ledoux, G.; Guillois, O.; Porterat, D.; Reynaud, C.; Huisken, F.; Kohn, B.; Paillard, V. *Phys. Rev. B* **2000**, *62*, 15942−15951.
(41) Pi, X. D.; Liptak, R. W.; Nowak, J. D.; Wells, N. P.; Carter, C. B.; Campbell, S. A.; Kortshagen, U. *Nanotechnology* **2008**, *19*, 245.